J Mater Sci (2011) 46:4690–4694
DOI 10.1007/s10853-011-5376-0

Proton conduction in $Ba_xCe_{0.8}Y_{0.2}O_{3-\alpha}$ + 0.04ZnO at intermediate temperatures and its application in ammonia synthesis at atmospheric pressure

Ming Zhang · Jia Xu · Guilin Ma

Received: 15 November 2010 / Accepted: 7 February 2011 / Published online: 24 February 2011
© Springer Science+Business Media, LLC 2011

Abstract Dense ceramic samples $Ba_xCe_{0.8}Y_{0.2}O_{3-\alpha} + 0.04ZnO$ ($x = 1, 0.98, 0.96, 0.94$) were successfully prepared by a solid-state reaction method, whose sintering temperature was about 573 K lower than a traditional solid state reaction method without sintering aid. XRD patterns indicated that all the samples exhibited a single-phase of orthorhombic perovskite structure. The conduction behavior was investigated by alternating current impedance in wet hydrogen atmosphere at 673–1073 K. It was found that the conductivities were affected by the nonstoichiometric amount of Ba, and increased in the order: σ ($x = 0.94$) $<$ σ ($x = 1$) $<$ σ ($x = 0.96$) $<$ σ ($x = 0.98$). It was also found that the samples were almost pure ionic conductors and contributed mainly by proton and partially by oxide ion in wet hydrogen atmosphere at 773–1073 K. The ammonia synthesis at atmospheric pressure was successfully conducted using an electrolytic cell based on $Ba_{0.98}Ce_{0.8}Y_{0.2}O_{3-\alpha} + 0.04ZnO$. The ammonia formation rate reached 2.36×10^{-9} mol s^{-1} cm^{-2} under the suitable conditions of 0.8 mA and 773 K.

Introduction

Protonic conductors with ABO_3-type perovskite structure, e.g., $SrCeO_3$ and $BaCeO_3$-based oxides, have a wide range of technological applications in solid oxide fuel cells (SOFCs), hydrogen sensors and ammonia synthesis at atmospheric pressure, etc. [1–6]. Among the proton-conducting oxides reported so far, barium cerate ceramics showed the highest proton conductivity, particularly when doped with 15–25 mol% Y, reached high conductivities around 10^{-2} S cm^{-1} at 873 K [7–9]. However, the sintering temperatures of such oxides were above 1873 K through a traditional solid state reaction method without sintering aid [9, 10]. Previous researches [11, 12] demonstrated that the addition of ZnO could significantly lower the sintering temperatures of $BaZr_{0.85}Y_{0.15}O_{3-\delta}$ and $BaCe_{0.5}Zr_{0.3}Y_{0.16}Zn_{0.04}O_{3-\alpha}$, respectively. Wang et al. [13] reported that when the addition of ZnO level was 4 mol%, the ceramic sample $BaCe_{0.5}Zr_{0.3}Y_{0.2}O_{2.9} + 0.04ZnO$ have both a high relative density (~98.5%) and a high-electrical conductivity (1.35×10^{-2} S cm^{-1} at 873 K). Guo et al. [14] and Xu et al. [15] successfully applied $BaZr_{0.4}Ce_{0.4}Y_{0.16}Zn_{0.04}O_{3-\alpha}$ and $BaCe_{0.5}Zr_{0.3}Y_{0.16}Zn_{0.04}O_{3-\alpha}$ in fuel-cell fabrication, respectively.

In addition, $BaCeO_3$-based proton conductors with nonstoichiometric Ba contents have aroused considerable interest [10, 16]. Ma et al. [10] synthesized and investigated nonstoichiometric $Ba_xCe_{0.9}Y_{0.1}O_{3-\alpha}$ ($x = 0.8$–1.2) ceramics, discovered that the sample of $x = 0.95$ showed both highest conductivity and better chemical stability.

To the best knowledge, there has been no report on 20 mol% Y^{3+} doped nonstoichiometric $BaCeO_3$, $Ba_xCe_{0.8}Y_{0.2}O_{3-\alpha}$, as of now. The aim of this study was to investigate the electrical conduction and the relationship between the conductivities and nonstoichiometry of $Ba_xCe_{0.8}Y_{0.2}O_{3-\alpha} + 0.04ZnO$ ($x = 1, 0.98, 0.96, 0.94$) ceramic samples in a wet hydrogen atmosphere in the intermediate temperature range of 673–1073 K. In addition, the authors applied $Ba_{0.98}Ce_{0.8}Y_{0.2}O_{3-\alpha} + 0.04ZnO$ ceramic sample which exhibited the highest conductivity to

M. Zhang · J. Xu · G. Ma (✉)
Key Laboratory of Organic Synthesis of Jiangsu Province,
College of Chemistry, Chemical Engineering and Materials
Science, Soochow University, Suzhou 215123, China
e-mail: 32uumagl@suda.edu.cn

ammonia synthesis at atmospheric pressure and investigated the influences of different conditions on the ammonia formation rate.

Experimental

The nonstoichiometric $Ba_xCe_{0.8}Y_{0.2}O_{3-\alpha} + 0.04ZnO$ ($x = 1, 0.98, 0.96, 0.94$) ceramic samples were prepared by a solid-state reaction method. Proper amounts of $Ba(CH_3COO)_2$, CeO_2, and Y_2O_3 were mixed with a agate mortar and pestle. The mixture was calcined in air at 1523 K for 10 h. The calcined powders were then mixed with an appropriate amount of ZnO, ball-milled for 3 h in ethanol, and then pressed into pellets at a hydrostatic pressure of 2.5×10^8 Pa and sintered at 1623 K for 10 h in air. The phase purities of the obtained ceramic samples were examined by a powder X-ray diffraction (XRD) on a Panalytical X′pert Pro MPD diffract meter with Ni filter using Cu K_α radiation. The morphologies of the ceramic samples were observed by a field-emission scanning electron microscopy (FESEM, Hitachi S-4700). The conductivities of the ceramic samples were measured by an AC-impedance method using electrochemical workstations (Zahner IM6EX) in the frequency range from 1 Hz to 3 MHz in wet hydrogen atmosphere at 673–1073 K. The ac signal strength was 50 mV. The flow rates for the humidified hydrogen were all 30 mL/min.

For the purpose of investigating the ionic conduction properties, hydrogen and water vapor concentration cells were constructed and the electromotive forces were measured at 773–1073 K. In wet hydrogen atmosphere, the observed electromotive force values (EMF_{obs}) of gas concentration cells were given by following Nernst equation [17, 18].

$$EMF_{obs} = \frac{RT}{2F}\left\{-t_{ion}\ln\left[p_{H_2(A)}/p_{H_2(B)}\right] + t_O\ln\left[p_{H_2O(A)}/p_{H_2O(B)}\right]\right\}$$

where $p_{H_2}(A)$, $p_{H_2O}(A)$, and $p_{H_2}(B)$, $p_{H_2O}(B)$ were partial pressures of hydrogen gases and water vapors in A, B gas chambers, respectively. If the p_{H_2O} in both cell chambers was the same, the electromotive force of the hydrogen concentration cell with $p_{H_2O}(A) = p_{H_2O}(B)$ gave the sum of the proton and oxide ion contributions. The ionic transport number ($t_{ion} = t_H + t_O$) was given by EMF_{obs}/EMF_{cal}, where EMF_{cal} was calculated from equation as follows:

$$EMF_{cal} = \frac{RT}{2F}\ln\left[p_{H_2(A)}/p_{H_2(B)}\right]$$

Similarly, the electromotive force of the water vapor concentration cell with $p_{H_2}(A) = p_{H_2}(B)$ gave the oxide ionic contribution. Therefore, the ionic transport number in wet hydrogen atmosphere may be evaluated by using the following concentration cells (1) and (2):

$$\begin{aligned}&H_2(p_{H_2}= 1.01 \times 10^5\text{Pa})\,(p_{H_2O} = 4.20 \times 10^3\text{Pa}),\\ &\quad Ag{-}Pd\,|Ba_xCe_{0.8}Y_{0.2}O_{3-\alpha}, + 0.04ZnO|Ag{-}Pd,\\ &\quad H_2{-}Ar\,(p_{H_2} = 1.01 \times 10^4\text{ Pa})\,(p_{H_2O} = 4.20 \times 10^3\text{ Pa})\end{aligned} \tag{1}$$

$$\begin{aligned}H_2(p_{H_2} &= 1.01 \times 10^5\text{ Pa})\,(p_{H_2O}\\ &= 7.40 \times 10^3\text{ Pa}),\ Ag{-}Pd\,|Ba_xCe_{0.8}Y_{0.2}O_{3-\alpha}\\ &\quad + 0.04ZnO|\ Ag{-}Pd,\ (p_{H_2}\\ &= 1.01 \times 10^5\text{ Pa})\,(p_{H_2O} = 4.20 \times 10^3\text{ Pa})\end{aligned} \tag{2}$$

In order to verify the proton conduction in the samples directly, a hydrogen pumping experiment [1] was performed by supplying direct current to the following electrolytic cell:

$$\begin{aligned}&\text{wet } H_2,\ Ag{-}Pd\ |\ Ba_xCe_{0.8}Y_{0.2}O_{3-\alpha} + 0.04ZnO\ |\\ &\quad Ag{-}Pd,\ \text{dry Ar}\end{aligned}$$

High purity hydrogen (99.999%) saturated with water vapor at room temperature was used as anode gas. High purity argon (99.999%) was dried using a liquid nitrogen sub cooler (about 153 K) and passed through the cathode chamber to carry the generated hydrogen gas to a gas chromatograph (Shanghai, GC-1650), where the amount of hydrogen gas in mixed gas was determined.The electrolytic cell for ammonia synthesis at atmospheric pressure was constructed:

$$\begin{aligned}&\text{wet } H_2,\ Ag{-}Pd\ |\ Ba_{0.98}Ce_{0.8}Y_{0.2}O_{3-\alpha} + 0.04ZnO\ |\\ &\quad Ag{-}Pd,\ \text{dry } N_2(-)\end{aligned}$$

The weight percent of Pd in Ag–Pd alloy was 25%. In the alloy, palladium may exhibit excellent catalytic activity for the reaction of ammonia synthesis [5], whereas silver may be of both desirable conduction and a synergy effect in this Ag–Pd alloy, which is similar to the Au–Pd alloy applied to catalyze direct oxidation of methane to methanol [19]. Pure hydrogen gas at 1 atm was introduced into the anode chamber and dry pure N_2 gas (dried by a liquid nitrogen sub cooler) was introduced into the cathode chamber. The flow rates of the two gases were all 30 mL/min. While a direct current was applied to the cell, ammonia evolved at the cathode was absorbed by 10 mL dilute sulfuric acid, and then the concentration of NH^{4+} was analyzed by spectrophotometry [20].

Results and discussion

Figure 1 shows the XRD patterns of $Ba_xCe_{0.8}Y_{0.2}O_{3-\alpha} + 0.04ZnO$ ($x = 1, 0.98, 0.96, 0.94$) ceramic samples sintered at 1623 K for 10 h. All samples have formed

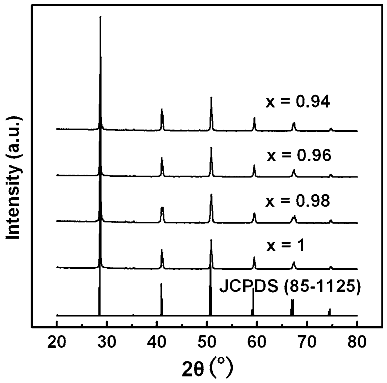

Fig. 1 X-ray powder diffraction patterns of sintered $Ba_xCe_{0.8}Y_{0.2}O_{3-\alpha}$ + 0.04ZnO ($x = 1, 0.98, 0.96, 0.94$)

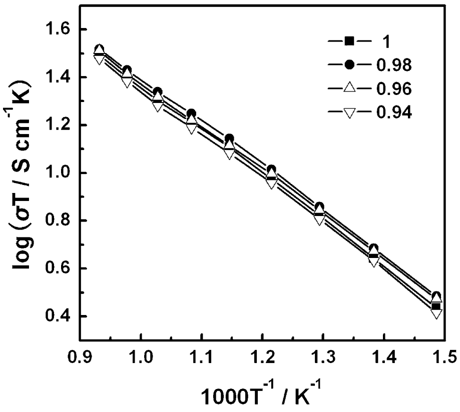

Fig. 2 Conductivities of $Ba_xCe_{0.8}Y_{0.2}O_{3-\alpha}$ + 0.04ZnO ($x = 1, 0.98, 0.96, 0.94$) in wet hydrogen

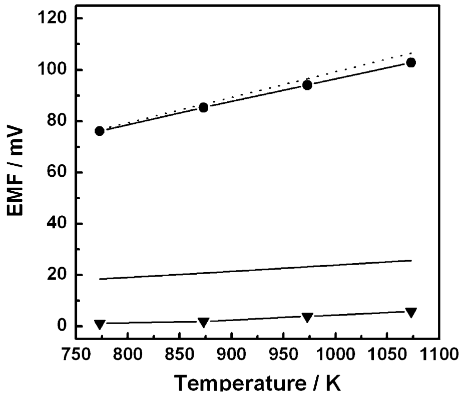

Fig. 3 The electromotive forces of hydrogen and water vapor concentration cells using $Ba_{0.98}Ce_{0.8}Y_{0.2}O_{3-\alpha}$ + 0.04ZnO. Dotted line and symbol filled circle represent the theoretical and the observed electromotive force values of the hydrogen concentration cell, respectively. Solid line and symbol inverted black triangle represent the theoretical and the observed electromotive force values of the water vapor concentration cell, respectively

a single orthorhombic perovskite structure. There was no visible pore on the surface and on cross section as confirmed by FESEM. The relative densities of all samples were higher than 96%. These results revealed that $Ba_xCe_{0.8}Y_{0.2}O_{3-\alpha}$ could be effectively sintered at 1623 K, which was about 573 K lower than the traditional solid-state reaction method without sintering aid [9, 10], by addition of 4 mol% ZnO.

Figure 2 shows the dependence of conductivities of $Ba_xCe_{0.8}Y_{0.2}O_{3-\alpha}$ + 0.04ZnO ($x = 1, 0.98, 0.96, 0.94$) ceramic samples on Ba content, x, in a wet hydrogen atmosphere at 673–1073 K. The conductivities of the ceramic samples increased in the order: σ ($x = 0.94$) < σ ($x = 1$) < σ ($x = 0.96$) < σ ($x = 0.98$). The sample of $x = 0.98$ showed the highest conductivity with a value of 1.59×10^{-2} S cm^{-1} in wet hydrogen at 873 K. Similar to $Ba_xCe_{0.9}Y_{0.1}O_{3-\alpha}$ with deficiency of Ba^{2+} [10], $Ba_{0.98}Ce_{0.8}Y_{0.2}O_{3-\alpha}$ + 0.04ZnO may also have such defect structure: some Y^{3+} ions transferred from Ce^{4+} to Ba^{2+} sites and occupied partial Ba^{2+} vacancies, but still left the Ba^{2+} vacancies and the corresponding O^{2-} vacancies. As a result, the oxygen vacancy concentration α in the sample of $x = 0.98$ was greater than that in the sample of $x = 1$, which helped to improve the ionic conductivities.

The electromotive forces of hydrogen and water vapor concentration cells using $Ba_{0.98}Ce_{0.8}Y_{0.2}O_{3-\alpha}$ + 0.04ZnO as electrolyte are plotted vs temperature in Fig. 3. As can be seen, the observed values were close to the corresponding theoretical values of hydrogen concentration cell. The calculated ionic transport numbers ($t_{ion} = 0.96$–0.99) were close to unity, the rest were electronic transport numbers ($t_e = 0.01$–0.04), indicating that the sample was almost a pure-ionic conductor. The oxide ionic (t_O) and protonic transference numbers ($t_H = t_{ion} - t_O$) were evaluated from the water vapor as well as the hydrogen concentration cells shown in Fig. 3 to be 0.06–0.22 and 0.93–0.74, respectively, indicated that the conduction was contributed mainly by proton and partially by oxide ion in wet hydrogen atmosphere at 773–1073 K.

According to Figs. 2 and 3, the partial conductivities of the various charge carriers of the $Ba_{0.98}Ce_{0.8}Y_{0.2}O_{3-\alpha}$ + 0.04ZnO in wet hydrogen atmosphere can be calculated and the results are shown in Fig. 4. The ionic conductivities were much higher than electronic conductivities, indicating the sample was almost a pure ionic conductor in wet H_2. The proton conductivities ($0.87 \times 10^{-2} - 2.38 \times 10^{-2}$ S cm^{-1}, at 773–1073 K) were higher than oxygen conductivities ($5.58 \times 10^{-4} - 6.84 \times 10^{-3}$ S cm^{-1}, at 773–1073 K).

In order to prove the proton conduction in the ceramic samples directly, the electrochemical hydrogen permeation was performed. The electrochemical hydrogen permeation rates of the representative sample are shown in Fig. 5.

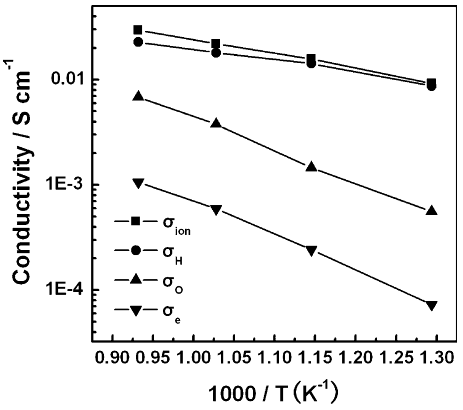

Fig. 4 Partial conductivities of the various charge carriers of the $Ba_{0.98}Ce_{0.8}Y_{0.2}O_{3-\alpha}$ + 0.04ZnO in hydrogen atmosphere

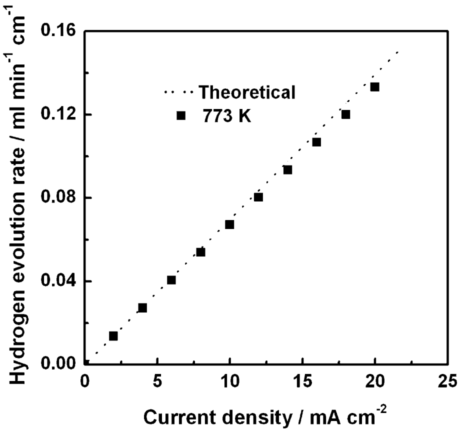

Fig. 5 Electrochemical hydrogen permeation rate of $Ba_{0.98}Ce_{0.8}Y_{0.2}O_{3-\alpha}$ + 0.04ZnO

In the hydrogen pump operated at 773 K, the evolution rate of hydrogen at the cathode deviated from that calculated from Faraday's law on sending a high current (>10 mA cm^{-2}) may because of some electronic conductivity created from the polarization under large current density conductions [21]. However, under a low current (<10 mA cm^{-2}), $t_H \approx 1$, indicated that the sample was almost a pure proton conductor under wet hydrogen atmosphere at 773 K. The other samples also exhibited similar phenomena.

Ammonia was synthesized through an electrolytic cell using $Ba_{0.98}Ce_{0.8}Y_{0.2}O_{3-\alpha}$ + 0.04ZnO as an electrolyte which has the highest proton conductivity. As shown in Fig. 6a, the ammonia formation rate increased with increasing temperature and reached a maximum (2.36 × 10^{-9} mol s^{-1} cm^{-2}) at 773 K, and then decreased with further increasing temperature. As shown in Fig. 6b, the ammonia formation rate increased with increasing applied current and then almost invariable after about 0.8 mA. The authors can see from Fig. 6c that the current efficiency became lower rapidly after about 0.8 mA. This resulted from that nitrogen chemisorption was hindered by the high rate of H$^+$ supply on the electrode surface, which poisoned the catalyst on the cathode surface, resulting in the decrease of the ammonia formation rate [22, 23]. Giving attention to Fig. 6a–c, the suitable conditions for the ammonia synthesis at atmospheric pressure were 0.8 mA and 773 K. The ammonia formation rate under the conditions was 2.36 × 10^{-9} mol s^{-1} cm^{-2}.

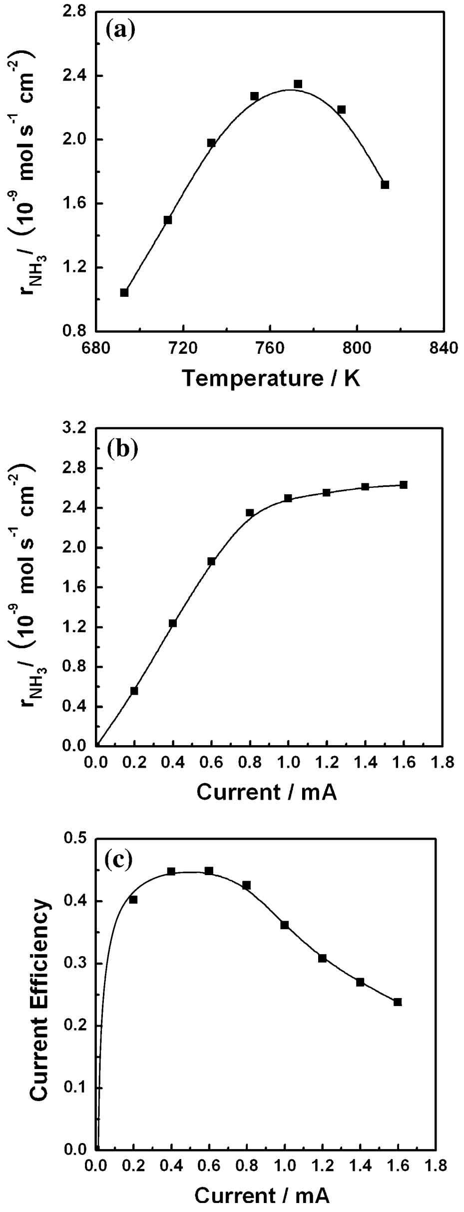

Fig. 6 The relationships between the ammonia formation rate and **a** operating temperature, **b** direct current applied for the electrolytic cell using $Ba_{0.98}Ce_{0.8}Y_{0.2}O_{3-\alpha}$ + 0.04ZnO; **c** the relationships between current efficiency and the imposed current at 773 K

The ammonia formation rate under the suitable conditions in this study was close to 2.1 × 10^{-9} mol s^{-1} cm^{-2} using $BaCe_{0.85}Y_{0.15}O_{3-\alpha}$ reported by us [8]. The result indicated that the addition of ZnO made no detrimental impact on the performance of sample.

Conclusions

The dense ceramic samples $Ba_xCe_{0.8}Y_{0.2}O_{3-\alpha} + 0.04ZnO$ ($x = 1$, 0.98, 0.96, 0.94) with a single orthorhombic perovskite structure were prepared by a solid-state reaction method. The sintering temperatures of the samples by addition of 4 mol% ZnO were about 573 K lower than the traditional solid state reaction method without sintering aid. Among all ceramic samples, the sample of $x = 0.98$ showed the highest conductivity with a value of 1.59×10^{-2} S cm^{-1} in wet H_2 at 873 K. The samples were almost pure ionic conductors and the ionic conduction was contributed mainly by proton and partially by oxide ion in hydrogen atmosphere at 773–1073 K. The sample of $x = 0.98$ was successfully applied to the ammonia synthesis at atmospheric pressure. The ammonia formation rate under the suitable conditions of 0.8 mA and 773 K was 2.36×10^{-9} mol s^{-1} cm^{-2}.

Acknowledgement This study was supported by the National Natural Science Foundation of China (no. 20771079).

References

1. Iwahara H, Esaka T, Uchida H, Maeda N (1981) Solid State Ionics 3–4:359
2. Iwahara H (1996) Solid State Ionics 86–88:9
3. Peng RR, Wu Y, Yang LZ, Mao ZQ (2006) Solid State Ionics 177:389
4. Kreuer KD (1996) Chem Mater 8:610
5. Marnellos G, Stoukides M (1998) Science 282:98
6. Liu JW, Li YD, Wang WB, Wang HTFZ, Ma GL (2010) J Mater Sci 45:5860. doi:10.1007/s10853-010-4662-6
7. Chiodelli G, Malavasi L, Tealdi C, Barison S, Battagliarin M, Doubova L, Fabrizio M, Mortalo C, Gerbasi R (2009) J Alloy Compd 470:477
8. Guo YX, Liu BX, Yang Q, Chen C, Wang WB, Ma GL (2008) Electrochem Commun 11:153
9. Tomita A, Hibino T, Suzuki M, Sano M (2004) J Mater Sci 39:2493. doi:10.1023/B:JMSC.0000020015.80430.d8
10. Ma G, Shimura T, Iwahara H (1998) Solid State Ionics 110:103
11. Babilo P, Haile SM (2005) J Am Ceram Soc 88:2362
12. Tao SW, Irvine JTS (2006) Adv Mater 18:1581
13. Wang H, Peng RR, Wu XY, Hu JL, Xia CR (2009) J Am Ceram Soc 92:2623
14. Guo YM, Ran R, Shao ZP (2010) Int J Hydrogen Energy 35:5611
15. Xu J, Lu XY, Ding YZ, Chen YH (2009) J Alloy Comp 488:208
16. Haile SM, Staneff G, Ryu KH (2001) J Mater Sci 36:1149. doi:10.1023/A:1004877708871
17. Shimura T, Esaka K, Matsumoto H, Iwahara H (2002) Solid State Ionics 149:237
18. Guan J, Dorris SE, Balachandran U, Liu M (1997) Solid State Ionics 100:42
19. Tomita A, Nakajima J, Hibino T (2008) Angew Chem Int Edit 120:1484
20. Zhang F, Yang Q, Pan B, Xu R, Hong HT, Ma GL (2007) Mater Lett 61:4144
21. Zhang F, Sun LL, Zhu JL, Pan B, Xu R, Ma GL (2008) J Mater Sci 43:1587. doi:10.1007/s10853-007-2328-9
22. Ouzounidou M, Skodra A, Kokkofitis C, Stoukides M (2007) Solid State Ionics 178:153
23. Wang WB, Cao XB, Gao WJ, Zhang F, Wang HT, Ma GL (2010) J Membrane Sci 360:397